# Slow interfacial reamorphization of Ge films melted by ps laser pulses

J. Siegel, J. Solis, and C. N. Afonso

Citation: J. Appl. Phys. **84**, 5531 (1998); doi: 10.1063/1.368598
View online: http://dx.doi.org/10.1063/1.368598
View Table of Contents: http://jap.aip.org/resource/1/JAPIAU/v84/i10
Published by the American Institute of Physics.

# Slow interfacial reamorphization of Ge films melted by ps laser pulses

J. Siegel,[a] J. Solis, and C. N. Afonso
*Instituto de Optica, CSIC, Serrano 121, 28006 Madrid, Spain*

(Received 19 May 1998; accepted for publication 20 August 1998)

Melting and rapid solidification is induced in 50-nm-thick amorphous Ge films on glass substrates by single laser pulses at 583 nm with a duration of 10 ps. The solidification process is followed by means of reflectivity measurements with ns time resolution both at the air/film (front) and the substrate/film (back) interfaces. Due to interference effects between the light reflected at the film–substrate and film–liquid interfaces, the back side reflectivity measurements turn out to be very sensitive to the melt depth induced by the laser pulse and their comparison to optical simulations enables the determination of the solidification dynamics. For low fluences, only a thin layer of the film is melted and solidification occurs interfacially leading to reamorphization of the molten material. The results provide a critical interface velocity for amorphization of ~4 m/s, much slower than the one that has widely been reported for elementary semiconductors. For high fluences, the molten layer depth approaches the film thickness and the results are consistent with a bulk solidification process. In this case, recalescence effects upon solid phase nucleation become important and lead to the formation of crystallites distributed throughout the whole resolidified volume. © *1998 American Institute of Physics.* [S0021-8979(98)05822-8]

## I. INTRODUCTION

The interest in the relation between the amorphous, liquid, and crystalline phases of elementary semiconductors has promoted a large amount of experimental and theoretical work.[1–3] Much effort has been expended investigating the different solidification scenarios occurring for different supercoolings and quench rates. The study of rapid solidification processes is one of the basic tools[4] to better understand the formation of metastable phases and the thermodynamics of systems far away from thermodynamic equilibrium. From the application point of view, the phase transition between the amorphous and the crystalline state in elementary semiconductors is of special interest for the development of thin film transistors (TFT).[5]

Interfacial solidification consists of a liquid/solid interface moving towards the region of maximum temperature. This type of solidification has been shown to lead to amorphization in Si if the interface velocity exceeds ≈15 m/s,[6] or to crystallization for lower interface velocities,[6,7] fine-grained polycrystalline material with no specific orientation being found in the latter case. The interface velocity has been determined by measuring the transient conductance[6] or the transient reflectivity changes[7] induced by pulsed laser melting. For initially amorphous films, the latent heat released during solidification may contribute to melt more amorphous material, since its melting point is below the one of the crystalline material. This can have the effect that a buried melt front is driven into the amorphous material leaving polycrystalline material behind.[8]

In contrast to interfacial solidification, bulk solidification[1,2,9] is characterized by the formation of solid nuclei within a melt which is at homogeneous temperature. This means that nuclei form all over the isothermal liquid volume and grow until they reach a critical size, above which crystal growth takes place. The formation of these nuclei from pre-existent nucleants or induced by density fluctuations in the liquid determines the heterogeneous or homogeneous character of the nucleation process, respectively. In the former case, bigger crystals with a certain orientation are formed, while fine grained crystalline material with no preferred orientation is produced in the latter case.[9]

Real time reflectivity (RTR) measurements with ns resolution[1,10–12] are a powerful method to investigate laser pulse induced rapid solidification processes. In general, the reflectivity is measured at the side of the sample exposed to the laser pulse, although the weakly transmitting top molten layer—due to the metallic nature of liquid semiconductors—hinders the probing of the whole sample thickness. The propagation of a buried molten layer into depth can be detected in thick films by means of infrared (IR) probe beams[7] because this wavelength region is only weakly attenuated by the solid material. In thin films, the reflectivity can be measured at the backside (substrate/film interface) of a film grown on a transparent substrate, although this method has been scarcely reported in the literature.[13,14] The advantage of this technique is the fact that the solidification process can be followed without the signal being attenuated by the molten surface layer. Nevertheless, its use is limited to the investigation of films on transparent substrates.

In this work we present a study of rapid solidification dynamics of thin Ge films on glass substrates under ps laser pulse irradiation by means of front and backside RTR measurements. The latter turn out to be very sensitive to the induced melt depth and allow, in combination with optical simulations, a complementary spatial and temporal characterization of the solidification process.

[a]Electronic mail:jan@pinar1.csic.es

 

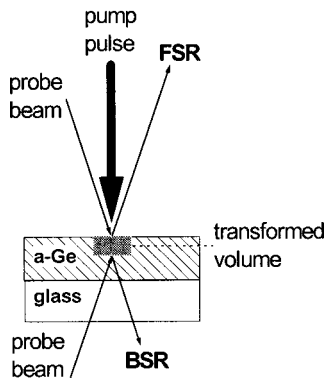


FIG. 1. Scheme of the front side reflectivity (FSR) and backside reflectivity (BSR) measurements. The thick arrow represents the ps laser pulse incident at the sample. The thin arrows show the beam path of the probing HeNe laser beams for the FSR and BSR modes of operation.

## II. EXPERIMENT

The samples investigated are 50 nm thick, very dense amorphous Ge films[15] sputtered at room temperature on glass substrates. The films are irradiated by single laser pulses of 10 ps at $\lambda = 583$ nm. The laser beam is focused onto the sample surface to a spot size with a diameter of about 0.5 mm corresponding to fluences up to 90 mJ/cm$^2$. The absolute fluence at the sample site is determined within 10% while the determination of the relative fluence difference between two different pulses can be done with an accuracy close to 2%. In all cases, the measurements are performed by exposing areas of the film to only one laser pulse. The transient reflectivity changes induced by the ps laser pulse are monitored by a HeNe laser ($\lambda = 633$ nm) focused to a size of 50 $\mu$m onto the center of the irradiated spot. Two classes of reflectivity transients are recorded as can be seen in Fig. 1. They are obtained by using the HeNe laser to monitor the reflectivity at the front and at the back side of the sample and will be referred to hereafter as front side reflectivity (FSR) and backside reflectivity (BSR) transients, respectively. The time resolution of the experiment is in both cases a few ns. Further details about the detection system and the laser system used can be found in Refs. 16, 17 and 10, 18, respectively.

In addition, optical simulations of the induced reflectivity changes were performed using two different computer programs designed for this purpose. The first program is based on the exact mathematical description of the interaction of an electromagnetic wave with an isotropic planar multilayered system formed by layers with different refractive indexes and absorption coefficients.[19,10] The calculation transforms layer by layer the optical constants of the initial material [amorphous Ge ($a$-Ge)][15] into the constants of the different phases involved in the process [liquid Ge (l-Ge)[20] or crystalline Ge (c-Ge)[15]] and calculates the reflectivity of the whole system at the monitoring wavelength as a function of the transformation depth. The program also considers the experimental angle of incidence (7°) and performs the calculations with a step size of 1 nm. In the case of bulk solidification, an accurate representation of the process should involve the conversion of the molten volume into crystallites distributed within an amorphous matrix. A good model is provided by effective-medium theories such as the one developed by Bruggemann[21] which is used here in a simulation program of the final reflectivity levels. It calculates the reflectivity of a solidified Ge film as a function of the crystalline fraction.

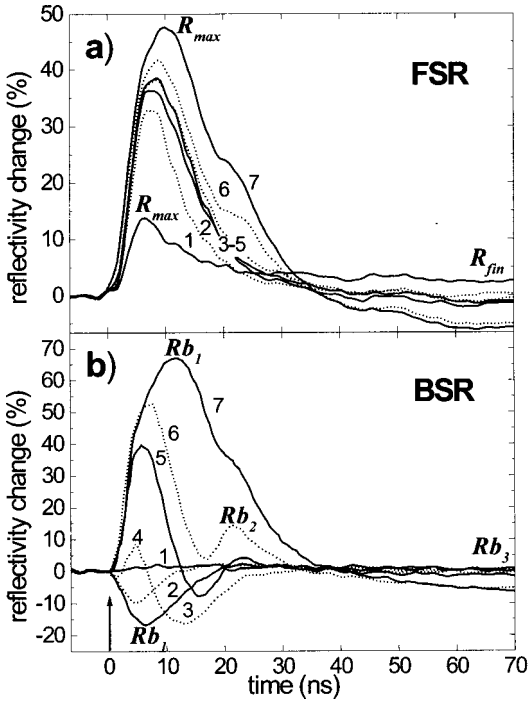


FIG. 2. Transient reflectivity changes in percent at 633 nm for $a$-Ge films irradiated with a ps laser pulse recorded in the (a) FSR and (b) BSR mode and at several fluences. The label numbers of the transients correspond to the following fluences: (1) 18, (2) 29, (3) 41, (4) 47, (5) 53, (6) 61, and (7) 72 mJ/cm$^2$. $R_{\max}$, $R_{\text{fin}}$, $R_{b1}$, $R_{b2}$, and $R_{b3}$ designate the characteristic reflectivity values of the transients. The temporal position of the laser pulse is marked by a vertical arrow in (b).

## III. RESULTS

### A. Reflectivity transients

We have recorded reflectivity transients at different fluences, using both FSR and BSR measurements. The transient reflectivity changes are expressed in percent according to $\Delta R = 100 * [R(t) - R_i]/R_i$, where $R(t)$ denominates the transient reflectivity value and $R_i$ the reflectivity value before irradiation. Figure 2 shows representative transients for each of the two types of reflectivity measurements performed [FSR in Fig. 2(a) and BSR in Fig. 2(b)]. Transients of different type but with the same number correspond to very similar fluences, so the corresponding FSR and BSR results can easily be correlated. The FSR transients are shown in Fig. 2(a), the results being very similar to those reported earlier.[10] The sharp reflectivity increase up to a maximum corresponds to film heating and melting and the amplitude of this reflectivity change reaches values close to 50% of the initial reflectivity, depending on the laser fluence. The subsequent decay to the final level is related to cooling and solidification. Above the melting threshold (20 mJ/cm$^2$), the maximum of the reflectivity increases strongly with laser fluence (transient $a2$). Then, over a quite large fluence range,

the amplitude of the transients changes only slightly (<3%), as can be seen in the transients $a3-a5$. For higher fluences, the initial maximum increases further (~10%) and a shoulder appears in the decreasing part of the transients ($a6$,$a7$) leading to a slow down of the decay process. The latter phenomenon is related to a temperature increase of the liquid due to the release of the solidification enthalpy upon nucleation of the solid phase and is usually referred to as recalescence.[1,2,10] This gives rise to the formation of crystalline material upon solidification as shown elsewhere,[10] in agreement with the lower level of the final reflectivity.

The corresponding BSR transients are shown in Fig. 2(b). Below the melting threshold, no reflectivity changes are observed (transient $b1$). Above the threshold, a slight reflectivity *decrease* takes place followed by a slow recovery (transient $b2$). The amplitude of this minimum increases reaching a value of ~17% below the initial sample reflectivity (transient $b3$) until an initial maximum is observed at a certain fluence, followed by the minimum which is shifted to longer times (transient $b4$). For higher fluences, the initial maximum increases more and more in amplitude and width and the subsequent minimum shifts to longer times decreasing its amplitude (transient $b5$). Increasing the fluence further, the minimum is followed by a second maximum smaller than the first one to reach smoothly the final level (transient $b6$). This second maximum is related to the recalescence process during film solidification since it appears whenever a shoulder is observed in the FSR transients. The final level observed now is clearly lower than the initial one indicating the formation of crystalline material upon solidification. Just before ablation occurs, both maxima have increased their width and amplitude such that the intermediate minimum is barely perceivable (transient $b7$). The first maximum corresponds now to a reflectivity increase of nearly 70%.

The comparison between FSR and BSR transients shows that only transients $a7$ and $b7$ are similar. While the FSR transients $a3-a5$ did not show any remarkable differences, the behavior of the corresponding BSR transients $b3-b5$ changes from a clear minimum to a high maximum followed by an oscillation below the initial level and a subsequent small second maximum. This is a clear indication of the depth sensitivity of the BSR technique since it reveals features which cannot be seen by the FSR measurements.

The maximum ($R_{\max}$) and the final reflectivity ($R_{\text{fin}}$) values measured at the FSR transients are shown in Fig. 3(a). The relative reflectivity changes measured in the transients have been converted into absolute reflectivity values using the optical constants reported elsewhere[15] to calculate the initial reflectivity of the sample. The precision of these characteristic values is within the symbol size. The melting threshold, defined by $R_{\max}$ values above the reflectivity of the solid at the melting point,[22] is found at 20 mJ/cm$^2$ and is followed by a sharp increase of $R_{\max}$ due to the metallic character of liquid Ge. A nearly saturated reflectivity level is reached for fluences around 40 mJ/cm$^2$. Above 54 mJ/cm$^2$ a slight additional increase can be observed, which coincides with the appearance of the shoulder in the transients due to recalescence. Even if the origin of this increase is not clear, it

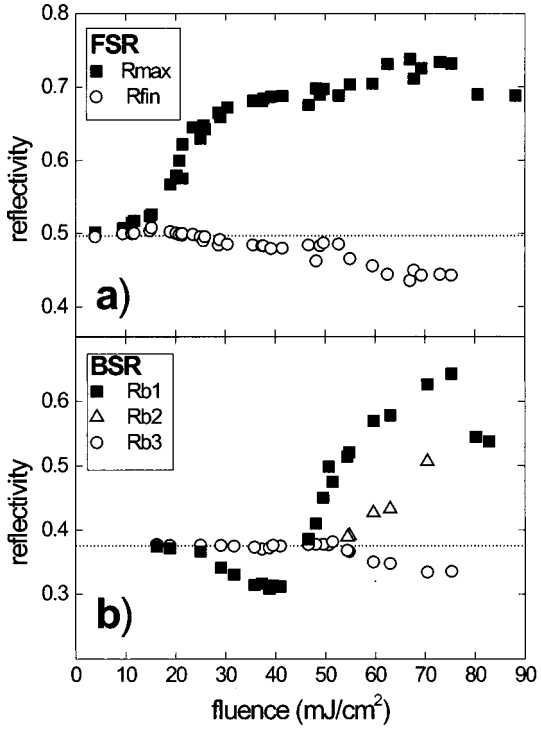


FIG. 3. Characteristic reflectivity values at 633 nm obtained from the transients in Fig. 2 and plotted as a function of the laser fluence for (a) FSR and (b) BSR transients. The dotted lines show the initial film reflectivity as calculated from its optical constants.

occurs at the same fluence at which $R_{\text{fin}}$ starts to decrease compared to the initial reflectivity value, evidencing the formation of crystalline material.[10] For fluences above 80 mJ/cm$^2$, ablation occurs as confirmed by visual inspection. For the case of BSR transients we have plotted in Fig. 3(b) as a function of fluence the reflectivity at the first extreme value ($R_{b1}$), which is a minimum for low fluences and a maximum for higher fluences, the reflectivity at the second maximum ($R_{b2}$) and the final level ($R_{b3}$). At about 25 mJ/cm$^2$, $R_{b1}$ appears in the form of an initial minimum which reaches its minimal value at about 40 mJ/cm$^2$. Fluences above 48 mJ/cm$^2$ give rise to an initial maximum whose reflectivity value ($R_{b1}$) is above that of the $a$-Ge film and increases rapidly with fluence. At 54 mJ/cm$^2$, the second maximum ($R_{b2}$) appears showing also an increase with fluence. Simultaneously with the appearance of a second maximum, the final reflectivity level ($R_{b3}$) begins to decrease reaching a final level well below the initial reflectivity value. This threshold, defined by the decrease of $R_{b3}$ and the appearance of $R_{b2}$ marks the onset of recalescence leading to film crystallization. Its position on the fluence scale is in perfect agreement with the simultaneous appearance of a shoulder in the FSR transients and a decrease of $R_{\text{fin}}$ [Fig. 3(a)].

### B. Optical simulations

Optical simulations corresponding to the FSR measurements are shown in Fig. 4(a), where the curve labeled l-Ge corresponds to the reflectivity of an $a$-Ge film on a glass substrate converting layer by layer into l-Ge, starting from the film/air interface. The l-Ge curve resembles the evolution

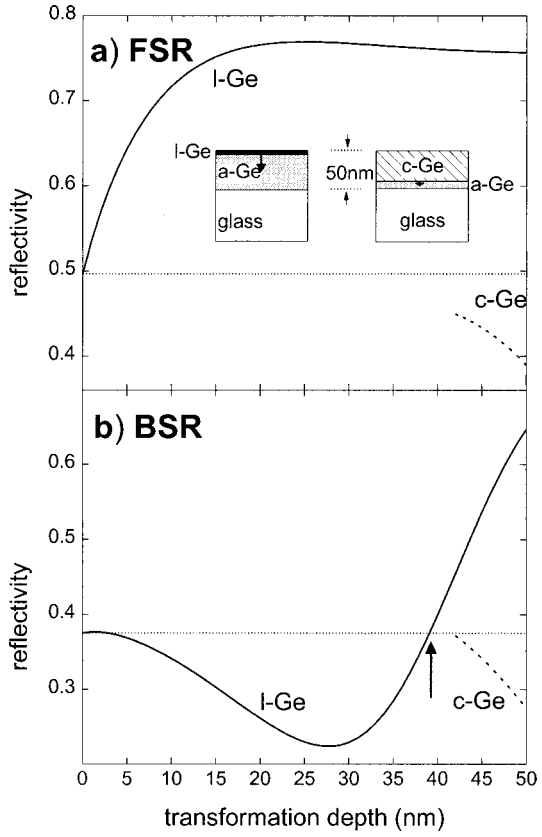


FIG. 4. Optical simulations of the evolution of the (a) FSR and (b) BSR as a function of the film transformation depth. The solid curves represent an *a*-Ge film converting layer by layer into l-Ge (see inset on the left hand side), and the dashed curves indicate the same type of conversion of the *a*-Ge film into *c*-Ge (see inset on the right hand side), both on top of a glass substrate. The latter curves have been simulated for a crystalline material thickness $\geqslant$42 nm, which is the minimum melt depth for which crystallization is observed. The dotted lines show the initial film reflectivity. The arrow in (b) emphasizes the fact that for any reflectivity value of the l-Ge curve above the dotted line, the melt depth is $\geqslant$40 nm.

of $R_{\max}$ in Fig. 3(a) and a comparison between both curves [Figs. 3(a) and 4(a)] provides an estimation of the melt depth induced for a given fluence. Accordingly, the experimental $R_{\max}$ value of 0.74 at the highest fluences reached should correspond to a melt depth of about 13 nm. This $R_{\max}$ value is nevertheless very close to the simulated one corresponding to a completely molten film (0.756). The flatness of the l-Ge curve in the range between 15 and 50 nm shows clearly that the FSR measurements are nearly insensitive to the melt depth changes induced at high fluences.

Figure 4(b) provides the simulation for the corresponding BSR measurements. The l-Ge curve shows now a clear decrease of reflectivity with increasing melt depth. It reaches its minimum when about half the film is melted. The origin of this behavior lies in the destructive interference of the light reflected at the interface glass/*a*-Ge with the light reflected at the *a*-Ge/l-Ge interface. Following the minimum, a steep increase takes place reaching a final reflectivity value of 0.647 for a completely molten film. The comparison with the corresponding experimental data of $R_{b1}$ in Fig. 3(b) shows that the reflectivity decrease starts to develop, as expected, immediately above the melting threshold indicating that the BSR is sensitive even to very shallow melt depths. The minimal value of $R_{b1}$ occurring at about 40 mJ/cm$^2$ should then correspond to a melt depth of $\sim$25 nm. According to the simulation, the transition of $R_{b1}$ to values higher than the initial level corresponds to a melt depth of $\sim$40 nm. The highest experimental value for $R_{b1}$ (0.64) is in perfect agreement with the simulated one for a fully molten film. As expected, BSR measurements are much more sensitive to the melt depth by the simple fact that—depending on the melt depth—they provide either a decrease or an increase of the reflectivity with respect to that of the as-deposited film. This assures that any $R_{b1}$ value above the initial level implies necessarily a melt depth of at least 40 nm. It is now clear that the actual melt depths are much greater than those estimated from the FSR measurements[10] due to the intrinsic lower sensitivity of the latter to melt depths greater than $\sim$13 nm [see Fig. 4(a)].

In order to analyze the behavior of the experimental final reflectivity level, i.e., that of the solidified material, simulations of a crystalline-amorphous bilayer (dashed curves) are also shown in Fig. 4. In this simulation, the depth of a crystalline top layer increases while the thickness of the whole system is considered to be constant (50 nm). Since below 54 mJ/cm$^2$ no crystallization takes place, the simulation starts from the melt depth induced at that fluence which can be estimated by comparing Figs. 3(b) and 4(b) giving a value of $\sim$42 nm. Although both simulated *c*-Ge curves resemble the decreasing behavior of the experimental $R_{\text{fin}}$ and $R_{b3}$ data (Fig. 3), the FSR *c*-Ge curve [Fig. 4(a)] predicts a reflectivity value at the crystallization threshold clearly below the initial one (dotted line) as opposed to the experimental data shown in Fig. 3(a). These results suggest that above the crystallization threshold solidification does not take place interfacially. In addition, and independently of the model, they ascertain that for a fully molten film ($\sim$74 mJ/cm$^2$) the resolidified material is not completely crystalline since the values of $R_{\text{fin}}$ and $R_{b3}$ do not reach the predicted levels.

## IV. DISCUSSION

In analyzing the present results it is important to keep in mind that the detection system used (ns resolution) can only follow accurately the film cooling and solidification processes since the heating induced by the pulse takes place in the ps range.[23,24] Lattice heating and melting occur during the absorption of the laser pulse thus leading to the *instantaneous*—as seen in the ns time scale—formation of a molten top layer of a certain thickness. The optical penetration depth in *a*-Ge at 583 nm is 23 nm[15] and the thickness of the molten layer is essentially defined by the exponential light absorption profile since the thermal conductivity of the film is low and consequently the thermal diffusion length during the pulse absorption is nearly negligible ($L_{\text{th}}$=4 nm).[25] Thus, the first extreme value of a transient corresponds to the initial melt depth. The measured values are slightly affected by the rise time of the detection system as observed for the maximal value of $R_{\max}$ (0.74) or the minimal value of $R_{b1}$ (0.30) which do not reach the values predicted by the simulations. From the initial situation on,

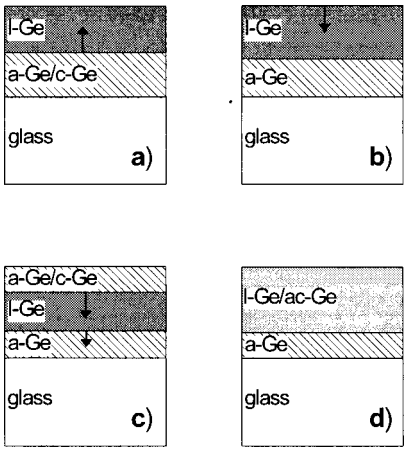


FIG. 5. Solidification scenarios of the *a*-Ge film following laser induced melting: (a) Interfacial solidification towards the surface (air/film). (b) Interfacial solidification initiated at the surface. (c) Interfacial solidification where a buried molten layer proceeds towards the substrate. (d) Bulk solidification of a molten layer.

the transients follow the reflectivity evolution of the sample during cooling and solidification, these processes occurring in the ns range.

Several solidification situations which could apply in our case are summarized in Fig. 5. While Figs. 5(a)–5(c) represent different interfacial solidification scenarios, Fig. 5(d) shows the situation for bulk solidification. Surely, the situations where solidification is surface initiated either (5b) moving downwards to the substrate or (5c) in form of a buried layer propagating in depth[26,27] are most unlikely because in these cases we should observe an oscillatory behavior (maxima and minima) in the FSR transients as we do for BSR transients. The scenario of an interfacial solidification towards the air/film interface is shown in situation 5a. In principle, it could explain qualitatively all types of transients observed *below the crystallization threshold*. This is supported by the fact the optical simulations in Fig. 4—assuming that type of solidification—resemble well the evolution of the experimental $R_{\max}$ and $R_{b1}$ values (Fig. 3).

The *temporal* evolution of the transients (below the crystallization threshold) can be also deduced from the simulated l-Ge curves as illustrated with the following example in the BSR transients. Since the $R_{b1}$ value of transient $b4$ [Fig. 2(b)] is above the initial reflectivity value, it corresponds to an initial melt depth of $\geqslant$40 nm on the l-Ge curve [arrow in Fig. 4(b)]. The temporal evolution of this transient during film solidification should follow now the l-Ge curve from this point to its left, i.e., reducing the melt depth to zero passing through a reflectivity minimum. This behavior is observed in the transient $b4$. Also the transients $b1-b5$ follow the l-Ge curve from their corresponding initial melt depth to its left. The same reasoning also applies for the FSR transients and the corresponding l-Ge curve. Only for those FSR and BSR transients obtained when recalescence effects are present, the temporal evolution cannot be deduced from the optical simulation thus indicating a different type of solidification.

The interface velocities during solidification can be estimated as the melt depth induced [obtained from the comparison of Figs. 3(b) and 4(b)] divided by the solidification time (obtained from Fig. 2). The values obtained range between 2 and 4 m/s, depending on the fluence. Even for low fluences when amorphization takes place, the estimated interface velocity never exceeds 4 m/s. This value is well below the minimum velocity reported ever in the literature for interfacial amorphization of elementary semiconductors.[6] However, those results refer to ns pulse irradiation of initially crystalline bulk Si and depend also on the crystal orientation (14 m/s for $\langle 111\rangle$ and 18 m/s for $\langle 100\rangle$).[28] Heat flow calculations for ns pulse irradiation of Si[29] provide similar values but do not include undercooling effects. The clear differences to our experimental conditions (initially amorphous material, substrate of low thermal conductivity, shorter pulse duration, and thus stronger undercooling) are responsible for the lower critical interface velocities for amorphization we measure. The interfacial character of the solidification process is strongly supported by the oscillatory behavior of the BSR transients and the fact that their evolution can be well simulated both *in time and in depth* by an interfacial model. Interfacial amorphization occurring at low velocities should be facilitated by the fact that the melt depth is smaller than the film thickness and the molten material is therefore in direct contact with amorphous material without seeds for crystallization, as distinct from the earlier studies on C–Si.[6]

Concerning the fluence regime at which crystallization occurs, we observed that the final reflectivity levels measured ($R_{\text{fin}}$ and $R_{b3}$ in Fig. 3) do not correspond to the ones obtained from interfacial simulations. In order to make an estimation of the induced crystalline fraction, a simulation of the final reflectivity level upon bulk solidification based on the effective-medium theory has been performed and the results are shown in Fig. 6. A comparison with the $R_{\text{fin}}$ and $R_{b3}$ values (Fig. 3) at high fluences gives in both cases a maximal crystalline fraction of $\approx$60%. Additionally, the decreasing behavior in both cases resembles well the behavior of the final levels observed experimentally above the crystallization threshold. The fact that the simulation results agree very well with the experimental data suggests that our assumption of a bulk solidification process taking place is correct.

A further convincing argument for bulk solidification to occur is the fact that the BSR and FSR transients ($a7/b7$ and probably also $a6/b6$) are essentially similar and no oscillatory behavior in their temporal evolution is observed, thus indicating a symmetric solidification situation. This can only happen in a bulk solidification scenario since an interfacial one would always give different and oscillatory FSR and BSR transients as it is evident from the simulations in Fig. 4.

The fact that we observe amorphization only for partially molten films and crystallization for (at least almost) completely molten films makes the amorphization threshold equal to the melting threshold and lower than the crystallization threshold. Sameshima *et al.*[2] reported that the threshold for amorphization of initially amorphous Si films on quartz was generally higher than the one for crystallization, concluding that only when the whole film was molten long enough to reduce the temperature gradient within the melt,

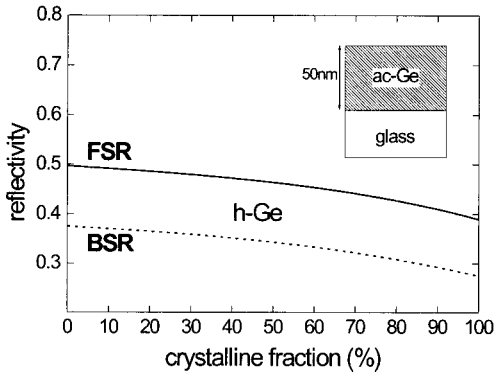


FIG. 6. Optical simulations of the evolution of the final reflectivity levels (FSR and BSR) for a simplified bulk solidification process. The curves provide the reflectivity evolution of a 50-nm-thick *a*-Ge film whose optical constants convert to those of *c*-Ge, as calculated by an effective-medium model developed by Bruggemann. The horizontal scale corresponds to the crystalline fraction.

the conditions for *amorphization via bulk solidification* could be achieved. We attribute the difference between their results and ours mainly to their longer laser pulse duration (30 ns) giving rise to a thermal diffusion length during the pulse absorption much bigger than the film thickness. This enables heat diffusion during the pulse duration, thus reducing the temperature gradient within the melt which is an indispensable condition for bulk solidification. In our case the thermal diffusion during the pulse is negligible and the molten volume is essentially defined by the exponential absorption profile causing a large temperature gradient. For low fluences (small melt depths) this is an ideal condition for interfacial solidification of the amorphous material which can occur even at extremely slow velocities (2–4 m/s), facilitated by the low thermal conductivity of the glass substrate.

In addition, Sameshima *et al.*[2] achieved complete amorphization only for Si films on glass substrate which were thinner than 24 nm, while they observed recalescence effects for thicker molten films leading to partial crystallization since more latent heat releases as the thickness of the molten layer increases. A minimal film thickness of 80 nm to observe recalescence has been recently reported by Vega *et al.*[30] for *a*-Ge films on Si substrates under ns laser pulse irradiation. Our results are in agreement with both works[2,30] in the sense that for increasing melt depths recalescence effects become strong enough to inhibit amorphization leading to the formation of some fraction of crystalline material. The different experimental conditions of the present work with respect to the references mentioned point out the major dependence of the solidification process on the heat flow conditions defined by the substrate, film thickness, and laser parameters (fluence, duration, and wavelength). In our case the results reveal a minimal thickness of ~42 nm of molten Ge to observe recalescence induced crystallization under ps pulse irradiation. Concerning the solidification scenario for such large melt depth, it is important to note that the temperature gradient is efficiently reduced by the high thermal diffusivity of liquid Ge[25] and at the same time the melt duration is increased due to the release of latent heat which dissipates only very slowly into the substrate of low thermal diffusivity. This forms the essential conditions for *bulk solidification* of the crystalline phase to take place.

## V. CONCLUSIONS

Real time reflectivity measurements performed through the substrate during laser induced melting and solidification of thin films proved to be a powerful technique for determining the solidification dynamics due to their sensitivity to the melt depth induced by the laser pulse. At low fluences reamorphization of Ge films occurs via interfacial solidification. For the first time interface velocities of less than 4 m/s leading to amorphization have been observed. This result points out the major influence of the heat flow conditions defined by the film, substrate, and laser parameters in addition to the absence of crystalline seeds. At high fluences, when recalescence induced crystallization takes place, the similarity of the reflectivity transients measured at the front and the back surface indicates clearly that bulk solidification is taking place. A minimum melt depth of about 42 nm for crystallization to occur is required and a maximum crystalline fraction of 60% induced upon solidification of a fully molten film is estimated.

## ACKNOWLEDGMENTS

Special thanks to J. M. Ballesteros for his work on the simulation program. We wish to thank also Dr. F. Vega (Dpto. Optica i Optometria, UPC, Barcelona, Spain) for the fruitful discussions during the elaboration of this work. Jan Siegel acknowledges the funding of the European Community through a grant (ERB40001GT954352) within the Training and Mobility of Researchers Program. This work has been partially supported by CICYT (Spain) under project TIC93-0125.

[1] S. R. Stiffler, M. O. Thompson, and P. S. Peercy, Appl. Phys. Lett. **56**, 1025 (1990).
[2] T. Sameshima and S. Usui, J. Appl. Phys. **74**, 6592 (1993).
[3] R. F. Wood and G. A. Geist, Phys. Rev. Lett. **57**, 873 (1986).
[4] W. Kurz and D. J. Fisher, *Fundamentals of Solidification*, 3rd ed. (Trans Tech, Switzerland, 1989).
[5] T. Sameshima, Appl. Surf. Sci. **96–98**, 352 (1996).
[6] M. O. Thompson, J. W. Mayer, A. G. Cullis, H. C. Webber, N. G. Chew, J. M. Poate, and D. C. Jacobson, Phys. Rev. Lett. **50**, 896 (1983).
[7] D. H. Lowndes, G. E. Jellison, Jr., S. J. Pennycook, S. P. Withrow, and D. N. Mashburn, Appl. Phys. Lett. **48**, 1389 (1986).
[8] R. F. Wood and G. A. Geist, Phys. Rev. Lett. **57**, 873 (1986).
[9] R. F. Wood, D. H. Lowndes, and J. Narayan, Appl. Phys. Lett. **44**, 770 (1984).
[10] J. Siegel, J. Solis, C. N. Afonso, and C. García, J. Appl. Phys. **80**, 6677 (1996).
[11] D. H. Auston, C. M. Surko, T. N. C. Venkatesan, R. E. Slusher, and J. A. Golovchenko, Appl. Phys. Lett. **33**, 437 (1978).
[12] G. E. Jellison, Jr., D. H. Lowndes, D. N. Mashburn, and R. F. Wood, Phys. Rev. B **34**, 2407 (1986).
[13] J. Boneberg, J. Nedelcu, H. Bender, and P. Leiderer, Mater. Sci. Eng., A **173**, 347 (1993).
[14] K. Murakami, O. Eryu, K. Takita, and K. Masuda, Phys. Rev. Lett. **59**, 2203 (1987).
[15] J. C. G. de Sande, C. N. Afonso, J. L. Escudero, R. Serna, F. Catalina, and E. Bernabeu, Appl. Opt. **31**, 6133 (1992).
[16] J. Solis and C. N. Afonso, J. Appl. Phys. **69**, 2105 (1991).
[17] J. Solis, F. Vega, and C. N. Afonso, Appl. Phys. A: Solids Surf. **62**, 197 (1996).

[18] J. Solis, J. Siegel, C. N. Afonso, J. Jimenez, and C. Garcia, J. Appl. Phys. **82**, 236 (1997).
[19] M. Born and E. Wolf, *Principles of Optics*, 6th ed. (Pergamon, Oxford, 1983), Chap. 1, p. 6.
[20] G. E. Jellison, Jr. and D. H. Lowndes, Appl. Phys. Lett. **51**, 352 (1987).
[21] D. A. G. Bruggemann, Ann. Phys. (Leipzig) **24**, 636 (1935); E. D. Palik, *Handbook of Optical Constants of Solids* (Academic, Orlando, 1985).
[22] J. Solis and C. N. Afonso, J. Appl. Phys. **72**, 2125 (1992).
[23] K. Sokolowski-Tinten, H. Schulz, J. Bialkowski, and D. von der Linde, Appl. Phys A: Solids Surf. **53**, 227 (1991).
[24] D. Agassi, J. Appl. Phys. **55**, 4376 (1984).
[25] W. Szysko, F. Vega, and C. N. Afonso, Appl. Phys. A: Solids Surf. **61**, 141 (1995).
[26] J. J. P. Bruines, R. P. M. van Hal, H. M. J. Boots, W. Sinke, and F. W. Saris, Appl. Phys. Lett. **48**, 1252 (1986).
[27] C. N. Afonso, J. Solis, J. Siegel, F. Vega, and W. Szyszko, Appl. Surf. Sci. **109/110**, 20 (1996).
[28] M. von Allmen, *Laser Beam Interactions with Materials* Springer Series in Materials Science Vol. 2 (Springer, Berlin, 1987).
[29] A. G. Cullis, H. C. Webber, N. G. Chew, J. M. Poate, and P. Baeri, Phys. Rev. Lett. **49**, 219 (1982).
[30] F. Vega, C. N. Afonso, W. Szyszko, and J. Solis, J. Appl. Phys. **82**, 1 (1997).